The Cytolytic P_{2Z} Receptor for Extracellular ATP Identified as a P_{2X} Receptor ($P2X_7$)

A. Surprenant,* F. Rassendren, E. Kawashima, R. A. North, G. Buell

The P_{2Z} receptor is responsible for adenosine triphosphate (ATP)–dependent lysis of macrophages through the formation of membrane pores permeable to large molecules. Other ATP-gated channels, the P_{2X} receptors, are permeable only to small cations. Here, an ATP receptor, the $P2X_7$ receptor, was cloned from rat brain and exhibited both these properties. This protein is homologous to other P_{2X} receptors but has a unique carboxyl-terminal domain that was required for the lytic actions of ATP. Thus, the $P2X_7$ (or P_{2Z}) receptor is a bifunctional molecule that could function in both fast synaptic transmission and the ATP-mediated lysis of antigen-presenting cells.

Extracellular ATP can permeabilize and lyse macrophages and related cells and may therefore have a role in cytolysis in the immune system (*1*,*2*); it is a candidate for the perforin- and Fas-independent cytolytic activity of T lymphocytes (*3*). On the basis of its unusual pharmacological properties, this action has been ascribed to activation of a receptor (P_{2Z}) that has been considered distinct from the other two classes of receptors for extracellular ATP, the P_{2X} and P_{2Y} receptors. The P_{2X} receptors are ligand-gated ion channels, and the P_{2Y} receptors are G protein–coupled receptors (*4*). The P_{2X} receptors form a family that is structurally distinct from other ligand-gated channels; six members ($P2X_1$ to $P2X_6$) that are encoded by distinct genes are currently known (*5*, *6*).

Here, we isolated a P2X receptor complementary DNA (cDNA) ($P2X_7$) that encodes a 595–amino acid protein (Fig. 1A) (*7*). The first 395 amino acids were 35 to 40% identical to those of the other six P_{2X} receptors, which are thought to have short intracellular NH_2- and COOH-termini, two transmembrane domains, and a large extracellular loop (*8*). The COOH-terminal domain of the $P2X_7$ receptor was much longer than that found in the other receptors but contained no further hydrophobic region that might span the membrane and showed no sequence homology with known proteins. The mRNA for the $P2X_7$ receptor was strongly expressed in J774 and P815 macrophages, in microglia, brain, spinal cord, lung, and spleen but was absent from thymus or the granulocytic RBL cell line (*9*).

Brief application (0.5 to 2 s) of ATP evoked inward currents in HEK 293 cells into which the $P2X_7$ receptor was transiently or stably transfected (Fig. 1B) (*10*). The agonist order of potency was BzATP ≫ ATP > 2MeSATP > ATP-γ-S ≫ ADP (Fig. 2, A and D) [where B_z is 2′ and 3′-(O)-(4-benzoyl benzoyl) and Me is methyl]; αβ-methylene ATP, βγ-methylene ATP, UTP, and adenosine were ineffective (concentration, 300 to 1000 μM). The removal of magnesium, calcium, or both from the external solution increased the amplitude of the current (Figs. 1B and 2A) and greatly prolonged the current, particularly when the applications were repeated. The increase in peak current (1.5- to 8-fold) was associated with little change in the half-maximal concentration (EC_{50}) (*11*); values for EC_{50} for BzATP and ATP were 7 ± 2 μM and 115 ± 9 μM in normal solution (n = 4) and 3.7 ± 0.7 μM and 85 ± 8 μM in zero magnesium (n = 7), respectively.

Currents with the same pharmacological profile were also recorded from J774 cells (Figs. 1C and 2, C and D). Antagonists had similar effects on J774 cells and HEK cells expressing the $P2X_7$ receptor: currents evoked by 30 μM BzATP were relatively insensitive to the purinoceptor antagonist suramin (15 to 38% inhibition with a concentration of 300 μM, n = 5) and moderately sensitive to the P_{2X} antagonist pyridoxalphosphate-6-azophenyl-2′,4′-disulfonic acid (half-maximal inhibition, 45 ± 8 μM in four HEK cells and 60 ± 9 μM in three J774 cells). Oxidized ATP (*12*) (100 μM) irreversibly blocked currents, provided cells were preincubated for 1 to 2 hours (n = 5); hexamethylene amiloride, which blocks the large pore formation at some P_{2Z} receptors (*2*), was ineffective (100 μM, n = 6) at blocking current. The $P2X_7$ receptor thus presents a pharmacological profile typical of the receptor previously termed P_{2Z} (*1*–*3*).

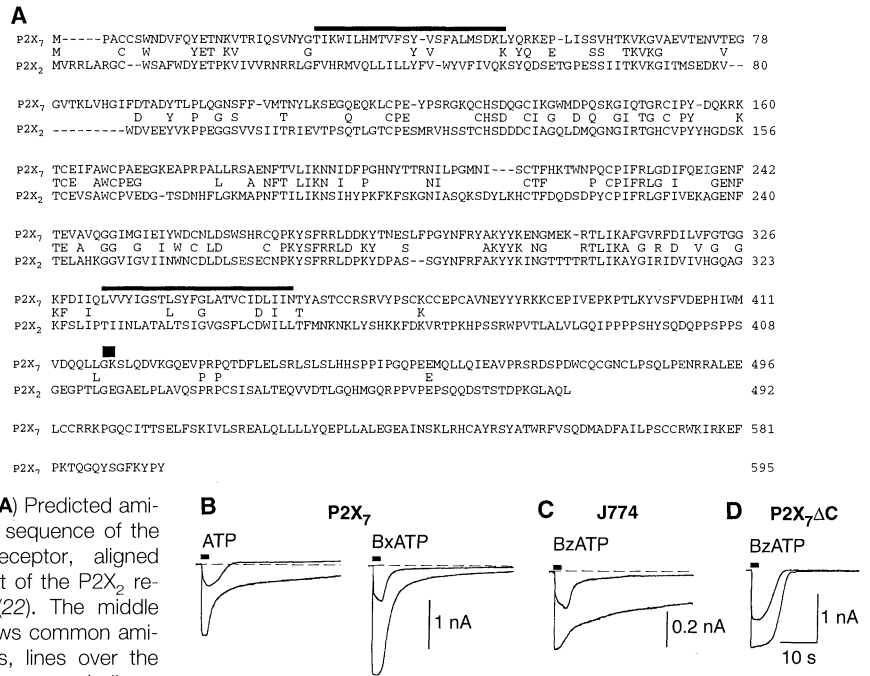

Fig. 1. (**A**) Predicted amino acid sequence of the $P2X_7$ receptor, aligned with that of the $P2X_2$ receptor (*22*). The middle line shows common amino acids, lines over the top sequence indicate probable membrane-spanning domains, and the square indicates the position of truncation. (**B**) ATP-induced currents in $P2X_7$ expressing HEK 293 cells are enhanced and prolonged by removal of magnesium. Currents were in response to 1-s applications of ATP (300 μM, left) and BzATP (right); the smaller of the two responses is in normal solution and the larger is in zero magnesium solution. (**C**) BzATP-induced currents in J774 cells; solutions with low concentrations of divalent cations also increased both amplitude and duration of the current. (**D**) BzATP-induced currents in HEK cells expressing $P2X_7\Delta C$; note that the low divalent solution increased the amplitude but not the duration of the currents. Current amplitude (mean ± SEM) to BzATP in normal solution from HEK cells transiently transfected with $P2X_7$ or $P2X_7\Delta C$ was 636 ± 118 pA and 590 ± 95 pA (n = 18), respectively. All recordings were from a holding potential of −70 mV; BzATP concentration was 30 μM in (B) through (D).

Glaxo Institute for Molecular Biology, Plan-les-Ouates, 1228 Geneva, Switzerland.

*To whom correspondence should be addressed. E-mail: AS28995@ggr.co.uk

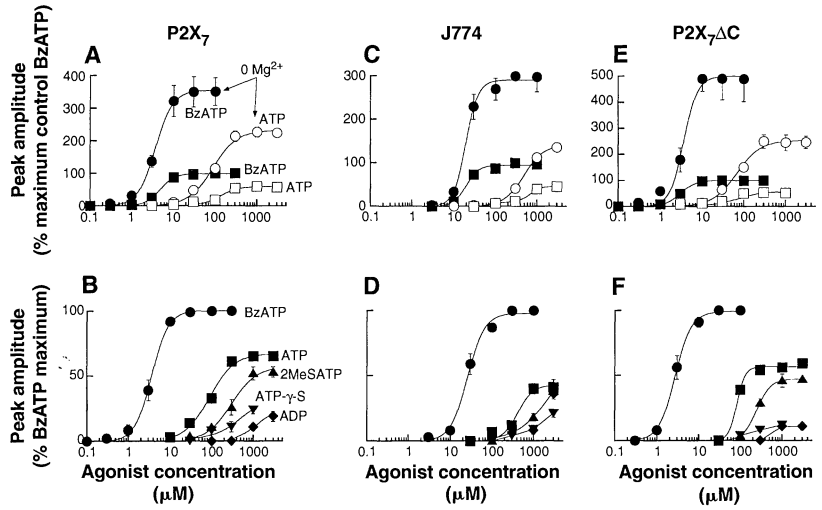

Fig. 2. Pharmacological properties of $P2X_7$ receptors, J774 macrophage cells, and $P2X_7\Delta C$ receptors. (**A**) Concentration-response curves for ATP (open symbols) and BzATP (closed symbols) in normal (squares) and low divalent (circles) external solution; results are plotted as the percent maximum response to BzATP in normal solution. (**B**) Concentration-response curves for ATP and ATP analogs (as indicated) in low divalent solution obtained from cells expressing the $P2X_7$ receptor. (**C** and **D**) Similar experiments on J774 cells; low divalent solutions also increased both amplitude and duration of the current. (**E** and **F**) Similar experiments on HEK cells expressing $P2X_7\Delta C$; all results were from a holding potential of −70 mV.

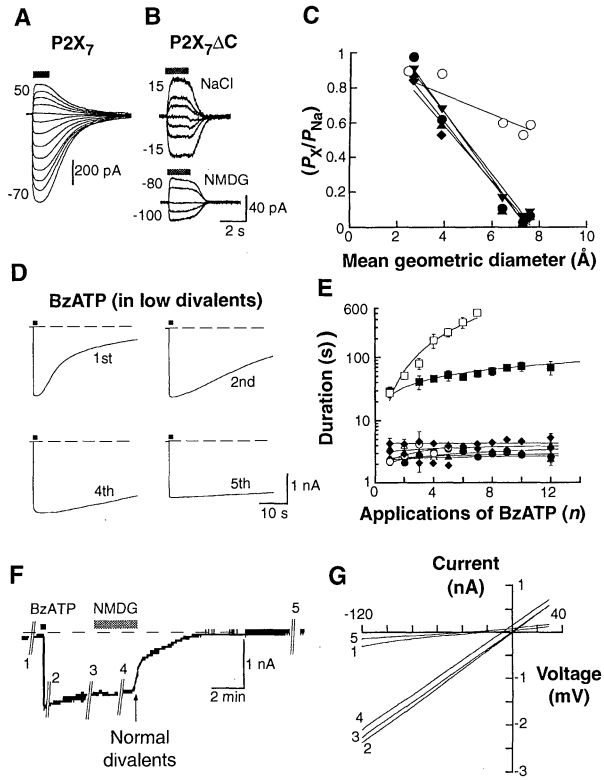

Fig. 3. At $P2X_7$ receptors, ATP activates currents that show selectivity for small cations (**A** through **C**) and also induces a sustained nonselective conductance [(D) through (G)]. In (A), superimposed currents are shown in response to 1-s application of BzATP at the holding potentials indicated (10-mV increments); normal external solution and internal solution contained cesium-aspartate. In (B) were similar experiments on HEK cells expressing the $P2X_7\Delta C$ receptor. Currents were evoked by BzATP at the holding potentials indicated (5-mV increments) in low external divalent solution containing 145 mM NaCl (top) or 145 mM NMDG (bottom). In (C), permeability ratios (P_X/P_{Na}) for some monovalent organic cations are plotted with their mean geometric diameter (*12*); data were derived from reversal potentials determined as shown in (A), (B), and (G). Filled symbols are for $P2X_7$ receptors (●) and J774 cells (▲) in normal solutions and for $P2X_7\Delta C$ (◆) and $P2X_2$ (▼) receptors in low divalent solutions. Open circles are for $P2X_7$ receptors in low divalent solutions. (**D** through **G**) Repeated applications of BzATP induced a sustained nonselective conductance. In (D), currents were recorded from HEK cells expressing $P2X_7$ receptor in response to four 1-s applications of BzATP, with an interval of 12 min between applications in low divalent solution throughout. In (E) is a summary from experiments as illustrated in (D); points are mean ± SEM (n = 6) exponential fits to the offset of the response, with a single exponential for $P2X_7\Delta C$ (◆) and $P2X_2$ (●) and a double exponential for $P2X_7$ (■). Filled symbols indicate normal concentrations of divalent cations; open symbols, low concentrations. In (F), maintained inward current was evoked by BzATP for 4 s. This application followed four prior applications (not shown); low divalent concentration was used throughout. The bar indicates the time during which the superfusing solution was changed from 145 mM NaCl to 145 mM NMDG (still in low concentrations of divalent cations). The arrow indicates the restoration of normal external solution. Breaks (1 to 5) indicate times of conductance measurement. In (G), current-voltage plots were obtained by ramp voltage commands at times 1 to 5 in (F). Note the very large conductance increase and the lack of effect of NMDG on the reversal potential [compare with (B)].

The BzATP-induced currents reversed polarity at −2 ± 0.3 mV (n =4); unlike currents at other P_{2X} receptors (*5*, *6*), they showed no rectification between −90 and 50 mV (Fig. 3A). The relative permeabilities of monovalent organic cations in the presence of external divalent cations were the same for $P2X_7$ receptors expressed in HEK cells and native J774 cells (*13*) and were not significantly different from those found previously for $P2X_2$ receptors (*14*) (Fig. 3C); the large cation *N*-methyl-D-glucamine (NMDG) was not significantly permeable (Fig. 3C). Reduction of the concentration of magnesium or calcium increased the current (Figs. 1B and 2A) but did not change the current-voltage relation, which was approximately linear (n = 5).

The P_{2Z} receptor has been characterized primarily by ion flux and dye uptake studies in macrophage-derived cell lines such as J774, particularly with the use of BzATP as the agonist and low extracellular divalent ion concentrations (*1*, *2*, *15*, *16*). We found a difference in the action of BzATP when the single brief applications were repeated in low concentrations of divalent cations (1 to 3 s duration with 30 μM BzATP at intervals of 2 to 15 min) (Figs. 3, D and E, and 4A). The currents declined much more slowly after each application, leading to sustained currents (Fig. 3, D and F) that reversed only very slowly (up to 20 min) when the agonist applications were stopped (*17*). However, the currents reversed within 1 to 3 min if the normal divalent cation concentration was restored (Figs. 3F and 4A). The conductance increase during the sustained current evoked by repeated applications of ATP (300 μM) or BzATP in a solution with a low concentration of divalent cations was almost nonselective among cations, with the cells becoming very permeable even to NMDG (Fig. 3, C, F, and G). The large molecular size (629 daltons) propidium dye YO-PRO-1 (*15*, *16*) could be seen to enter the cell during these recordings (Fig. 4A) (*18*). In separate experiments, we found that > 85% of stably transfected cells took up YO-PRO-1 during incubation with BzATP for 3 to 5 min in a solution with a low concentration of divalent cations (Fig. 4, D and E) (*18*).

In normal or reduced concentrations of divalent cations, repeated applications of ATP or BzATP did not induce such sustained currents in cells expressing other P_{2X} receptors (*19*) (Figs. 3E and 4C) and did not cause uptake of YO-PRO-1 by HEK cells expressing the $P2X_2$ receptor (Fig. 4, D through F). We tested the hypothesis that the unique COOH-terminal domain conferred these properties by repeating the experiments on HEK cells expressing the $P2X_7$ receptor truncated to 418 amino acids ($P2X_7\Delta C$, Fig. 1A). Agonist and antagonist actions at this $P2X_7\Delta C$ receptor were not

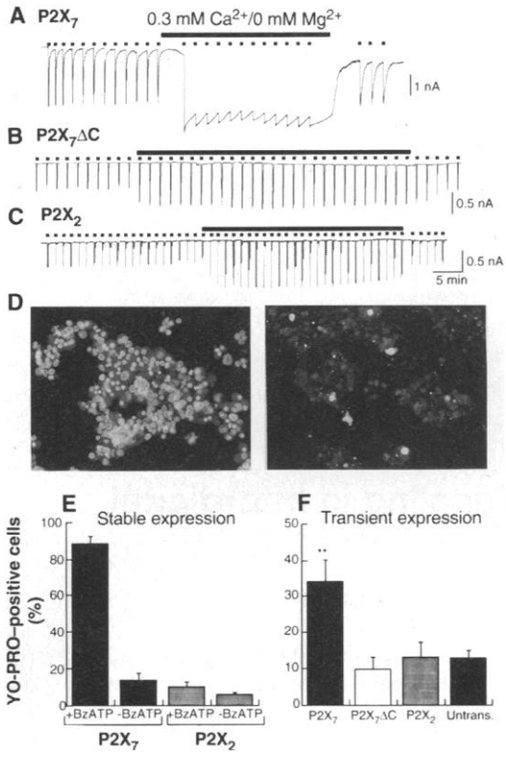

Fig. 4. Activation of $P2X_7$ receptors, but not of $P2X_7\Delta C$ receptors, induces a nonselective conductance and cytolysis. Shown are currents in HEK cells expressing $P2X_7$ (**A**), $P2X_7\Delta C$ (**B**), or $P2X_2$ (**C**) receptors during repeated applications (1 s each) of BzATP at 100-s intervals. During the time indicated, the external solution was changed from the normal solution to the low divalent solution. The concentration of BzATP was 30 μM in (A) and 300 μM in (B) and (C). YO-PRO-1 could be seen to enter the cell in low divalent solutions during recordings such as that shown in (A) (n = 8) but not during experiments as in (B) and (C) (n = 7). (**D**) Photomicrographs of HEK cells stably expressing $P2X_7$ (left) or $P2X_2$ (right) receptors after a 5-min incubation with YO-PRO-1 (10 μM) and BzATP (30 and 300 μM, respectively) in low divalent solution. (**E**) Summary of results from HEK cells stably expressing $P2X_7$ or $P2X_2$ receptors. (**F**) Summary of results from cells transiently expressing $P2X_7$, $P2X_7\Delta C$, $P2X_2$, or no receptors (Untrans.). BzATP concentration was 30 μM for experiments with the $P2X_7$ receptor and 300 μM for all others (n = 6 throughout).

different from those at wild-type receptors, and reduction of divalent cations increased the amplitude of the response at $P2X_7\Delta C$ receptors as at wild-type $P2X_7$ receptors (Figs. 1D and 2, E and F). However, in cells expressing the $P2X_7\Delta C$ receptor, solutions with low concentrations of divalent cations did not alter the kinetics of the response, the sustained current was not induced by repeated applications (Figs. 1D; 3, B, C, and E; and 4B), and no uptake of YO-PRO-1 was induced by BzATP (Fig. 4, E and F).

Thus, the expression of a single protein, the $P2X_7$ receptor, endows cells with two distinct responses to ATP and its analog BzATP. The first, a transient current through channels permeable to small cations and similar to responses at other P_{2X} receptors, is evoked by widely separated brief agonist applications. The second, a sustained current through a nonselective pore, leading to cell death, is evoked by repeated agonist applications, particularly in low concentrations of divalent cations. The second response requires the COOH-terminal domain. It is likely that these properties reside entirely in the expressed protein, such that distinct conformations result in a channel permeable to small cations or in a pore permeable to very large ions, leading to cytolysis. Alternatively, an interaction of the unique COOH-terminus with other proteins intrinsic to HEK 293 cells might confer the cytolytic properties of the $P2X_7$ receptor (2). Any such protein must be ubiquitous because we obtained qualitatively similar results from Chinese hamster ovary cells and nonmammalian *Spodopteria frugiperda* (Sf9) cells transiently expressing $P2X_7$ receptors (*20*).

P_2 receptors for extracellular ATP now fall into the same two classes seen for other hormones and transmitters; these are the G protein–coupled receptors with seven transmembrane domains (P_{2Y}) and the receptors with integral ion channels (P_{2X}) (*4*, *8*). Here, we have identified the P_{2Z} receptor as a member of the P_{2X} family. The dual function of the $P2X_7$ receptor, whereby it can operate both as an ion channel selective for small cations and in the induction of cell lysis, has an overall analogy with ionotropic glutamate receptors. These also function predominantly as ligand-gated ion channels involved in synaptic transmission, but for a subset of receptors, repeated or prolonged activation is neurotoxic because of excessive calcium influx (*21*). The induction of a lytic pore independent of calcium entry provides a novel mechanism through which transmitters can kill cells.

REFERENCES AND NOTES

1. H. P. Buisman *et al.*, *Proc. Natl. Acad. Sci. U.S.A.* **85**, 7988 (1988); A. Zambon *et al.*, *Cell. Immunol.* **156**, 458 (1994).
2. L. C. Nuttle and G. R. Dubyak, *J. Biol. Chem.* **269**, 13988 (1994).
3. D. K. Blanchard *et al.*, *Blood* **85**, 3173 (1995); F. DiVirgilio, P. Pizzo, P. Zanovello, V. Bronte, D. Collavo, *Immunol. Today* **11**, 274 (1990); C. C. Liu, C. M. Walsh, J. D. E. Young, *ibid.* **16**, 194 (1995).
4. C. Kennedy and P. Leff, *Trends Pharmacol. Sci.* **16**, 168 (1995); M. P. Abbracchio and G. Burnstock, *Pharmacol. Ther.* **64**, 445 (1995).
5. G. Collo *et al.*, *J. Neurosci.* **16**, 2495 (1996); A. J. Brake, M. J. Wagenbach, D. Julius, *Nature* **371**, 519 (1994); S. Valera *et al.*, *ibid.*, p. 516; C. Chen *et al.*, *ibid.* **377**, 428 (1995); C. Lewis *et al.*, *ibid.*, p. 432.
6. G. Buell, C. Lewis, G. Collo, R. A. North, A. Surprenant, *EMBO J.* **15**, 55 (1996).
7. A 440–base pair (bp) fragment of $P2X_7$ was amplified with inosine-containing degenerate oligonucleotides from several peripheral autonomic ganglia (*6*). Using this fragment as a hybridization probe, we isolated a partial $P2X_7$ cDNA from λgt10 prepared from rat superior cervical ganglia mRNA. This 3.5-kb cDNA was truncated at the 5′ end, beginning with the codon for amino acid residue 141, and did not have a polyadenylated [poly(A)$^+$] tail. We cloned an additional 468 bp of 5′ cDNA by rapid amplification of cDNA ends–polymerase chain reaction (RACE-PCR; Life Technologies, Bethesda, MD) using poly(A)$^+$ RNA from the medial habenula. $P2X_7$ receptor-specific sequences were amplified with two rounds of nested PCR, for which sense primers were CCACGCGTCGACTAGTACGGGIIGGGIIGGGIIG and GGAATTCCACGCGTCGACTAGTAC and antisense primers were GGCGTATCTGAAGTTGTAGC and GTCCAGCCGGCGGAAGCTGT. A shared restriction site (Bgl II) permitted ligation of the RACE-PCR product and of the partial cDNA, yielding a construct that encoded the entire $P2X_7$ protein. This chimera (GenBank accession number X95882) was expressed in pcDNA3 (Invitrogen, San Diego, CA), sequenced by fluorescent DNA sequencing (Perkin Elmer, Foster City, CA), and confirmed by isolation of other full-length $P2X_7$ cDNAs from a rat brain cDNA library (Clontech, Palo Alto, CA). One of these included a stop codon 130 bp upstream from the ATG. The COOH-terminus was removed by excision of a Xcm I–Not I fragment, and the resulting protein ($P2X_7\Delta C$) was $P2X_7(1–418)$.
8. A. Surprenant, G. Buell, R. A. North, *Trends Neurosci.* **18**, 224 (1995).
9. Digoxigenin-labeled antisense riboprobe was generated from the full-length $P2X_7$ cDNA and used for Northern (DNA) blotting on 300 ng of poly(A)$^+$ RNA of each sample that had been electrophoresed and transferred to nylon; hybridization was detected by chemiluminescence.
10. Whole-cell recordings were obtained at room temperature from HEK 293 cells transiently or stably transfected with $P2X_7$ cDNA, from HEK 293 cells transiently transfected with $P2X_7\Delta C$ cDNA, and from J774A.1 cells (American Type Culture Collection, Rockville, MD); agonists were applied for periods of 1 to 3 s by a fast-flow U-tube delivery system [E. M. Fenwick, A. Marty, E. Neher, *J. Physiol. (London)* **331**, 577 (1982)]. The internal pipette solution was 140 mM cesium-aspartate or potassium-aspartate, 20 mM NaCl, 10 mM EGTA, and 5 mM Hepes; normal external solution was 145 mM NaCl, 2 mM KCl, 2 mM $CaCl_2$, 1 mM $MgCl_2$, 10 mM Hepes, and 12 mM glucose. Low divalent external solution was nominally magnesium-free with 0.3 mM $CaCl_2$. For cells expressing $P2X_7$ receptors and J774 cells, we constructed concentration-response curves in low divalent solution by recording currents in response to 1-s applications of agonist at 8-min intervals with normal external solution present for 6 min before each application. This protocol was necessary to prevent the development of sustained inward currents (see Figs. 3 and 4). Lipofectin was used for transfection as described (*6*).
11. It has been suggested that ATP^{4-} is the active species at the P_{2Z} receptor (*2*). The three solutions used contained 2 mM $CaCl_2$ and 1 mM $MgCl_2$, 2 mM $CaCl_2$ and 0 mM $MgCl_2$, and 0.3 mM $CaCl_2$ and 0 mM $MgCl_2$; the concentrations of ATP^{4-} resulting from the addition of 100 μM Na-ATP to these solutions would be 3.7 μM, 5.1 μM, and 29 μM, respectively.
12. M. Murgia, S. Hanau, P. Pizzo, M. Rippa, F. DiVirgilio, *J. Biol. Chem.* **268**, 8199 (1993).
13. Reversal potentials (E_{rev}) were obtained by application of ATP (300 μM) or BzATP (30 μM) while the membrane was held at various potentials or by application of voltage ramps from −120 to 30 or 50 mV. We calculated permeability ratios from E_{rev} by

first computing α (= P_{Na}/P_K, where P is permeability) for internal (i) and external (o) concentrations $[Na]_i$ = 20 mM, $[Na]_o$ = 145 mM, $[K]_o$ = 0 mM, and $[K]_i$ = 140 mM from α = {[145/exp($E_{rev}F/RT$)] − 20}/140 (where F is the Faraday, R is the gas constant, and T is the absolute temperature). Other P_X/P_{Na} values, when $[X]_o$ = 145 mM, $[Na]_i$ = 20 mM, $[K]_i$ = 140 mM, and $[Na]_o$ = $[K]_o$ = $[X]_i$ = 0 mM, were computed from P_X/P_{Na} = {[exp($E_{rev}F/RT$)](20 + 140α)}/145. In order of size (Fig. 3C), X was cesium, methylamine, tris(hydroxymethyl)-aminomethane, tetraethylammonium, and *N*-methyl-D-glucamine. The internal solution also contained 10 mM EGTA and 5 mM Hepes. External solutions also contained 10 mM glucose and normal or low concentrations of divalent cations; pH was maintained at 7.3 with HCl, histidine, or Hepes as required, and the osmolarity of all solutions was 295 to 315.

14. R. J. Evans, *J. Physiol. (London)* **487**, 193P (1995).
15. S. E. Hickman, J. El-Khoury, S. Greenberg, I. Schieren, S. C. Silverstein, *Blood* **84**, 2452 (1994).
16. J. S. Wiley, J. R. Chen, M. B. Snook, G. P. Jamieson, *Br. J. Pharmacol.* **112**, 946 (1994); T. H. Steinberg, A. S. Newman, J. A. Swanson, S. C. Silverstein, *J. Biol. Chem.* **262**, 8884 (1987).
17. The induction and kinetics of this sustained current were the same for inward current at −70 mV and for outward current at 50 mV (n = 3). Indeed, it did not require any current to flow during the first, conditioning agonist applications: when BzATP was applied 4 to 12 times in normal divalent solution while the reversal potential was held (0 mV in NaCl or −90 mV in NMDG), the sustained current was still evoked by the subsequent application of BzATP when the low divalent solution was introduced and the holding potential was set to −70 mV (n = 3; A. Surprenant *et al.*, data not shown).
18. YO-PRO-1 (10 μM; Molecular Probes, Eugene, OR) was added to the superfusion fluid during electrophysiological recordings 3 to 6 min before switching to low divalent solution and washed out upon switching back to normal divalent solution, after which the fluorescent lamp was turned on and cells were examined with a fluorescein isothiocyanate filter. For cell counts, 500 cells per cover slip were counted in each case.
19. R. J. Evans *et al.*, *Mol. Pharmacol.* **48**, 178 (1995).
20. A. Surprenant *et al.*, data not shown.
21. D. W. Choi, *Neuron* **1**, 623 (1988).
22. Abbreviations for the amino acid residues are as follows: A, Ala; C, Cys; D, Asp; E, Glu; F, Phe; G, Gly; H, His; I, Ile; K, Lys; L, Leu; M, Met; N, Asn; P, Pro; Q, Gln; R, Arg; S, Ser; T, Thr; V, Val; W, Trp; and Y, Tyr.
23. We thank A. Brake and D. Julius for $P2X_2$ cDNA and M. J. Solazzo for sequencing. We are indebted to D. Estoppey for cell culture, transfections, and generating stable cell lines.

15 January 1996; accepted 2 April 1996

Requirement for BMP Signaling in Interdigital Apoptosis and Scale Formation

Hongyan Zou and Lee Niswander*

Interdigital cell death leads to regression of soft tissue between embryonic digits in many vertebrates. Although the signals that regulate interdigital apoptosis are not known, BMPs—signaling molecules of the transforming growth factor–β superfamily—are expressed interdigitally. A dominant negative type I BMP receptor (dnBMPR-IB) was used here to block BMP signaling. Expression of dnBMPR in chicken embryonic hind limbs greatly reduced interdigital apoptosis and resulted in webbed feet. In addition, scales were transformed into feathers. The similarity of the webbing to webbed duck feet led to studies that indicate that *BMP*s are not expressed in the duck interdigit. These results indicate BMP signaling actively mediates cell death in the embryonic limb.

Programmed cell death (PCD) or apoptosis is an important aspect of embryonic development. Significant progress has been made in defining the intracellular pathways of PCD [reviewed in (*1*)]; less well understood, however, are the extracellular events that trigger the process. Apoptosis can result from changes in the extracellular environment, such as alterations in cell adhesion or withdrawal of growth factors (*2*). Rather paradoxically, the presence of a growth factor, bone morphogenetic protein 4 (BMP4), has been suggested to mediate apoptosis of neural crest cells in the developing hindbrain of chickens (*3*).

In the developing chick limb, apoptosis occurs in the interdigital region, as demonstrated by vital dye uptake, nuclear fragmentation, DNA laddering, and TUNEL staining (*4, 5*). Recent studies indicate that interdigital apoptosis can be inhibited by peptide inhibitors of the protease family of intracellular CED-3–interleukin-1β converting enzyme (*6*). Possible extracellular signals of interdigital apoptosis include BMP2, BMP4, and BMP7, all of which are expressed in the interdigital tissue before and during regression in the developing mouse and chick limb bud (*7–11*).

We chose to look at the role of BMPs in limb development. One approach to study BMP function is to block BMP signaling at the level of the receptor. Two types of transmembrane serine-threonine kinase receptors are involved in signaling by BMP and other transforming growth factor–β (TGF-β) family members. Upon ligand binding, type II BMP receptor (BMPR-II) associates with type I BMPR (BMPR-I), and this interaction is essential for signal transduction (*12, 13*). By analogy with activation by TGF-β (*14*), it is thought that ligand-induced receptor association leads to phosphorylation of BMPR-I by BMPR-II and initiation of signal transduction by BMPR-I. Two type I BMPRs have been identified, BMPR-IA (ALK3) and BMPR-IB (ALK6). In in vitro binding assays, BMPR-IB (used in the studies reported here) specifically binds BMP2 and BMP4 and binds BMP7 with lower affinity. BMPR-IB does not bind TGF-β or activin (*15*).

A single amino acid substitution within the adenosine triphosphate binding site (K231R, where Lys^{231} is changed to Arg) was made to generate a dominant negative mutant form of mouse BMPR-IB (dnBMPR). The dnBMPR is inactive in an in vitro kinase assay and defective in signal transduction (*16, 17*). Moreover, excess mutant BMPR can compete with endogenous type I receptor for type II receptors and therefore can act as a dominant negative mutation. We chose to generate the single amino acid mutation rather than an intracellular deletion of the kinase domain for several reasons. (i) The K-to-R conservative substitution should not alter the overall conformation of the receptor. (ii) Cellular trafficking of the K231R receptor should not be disrupted, as often happens for intracellular deletion mutations. (iii) Point mutations should not alter the strong interaction between the intracellular domains of the type I and II BMP receptors (*12*).

The mutant receptor construct was cloned into an avian replication-competent retroviral vector (RCAS) (*18*) and used to produce high-titer viral stock (*19*). The virus was microinjected into the region of the right presumptive hind limbs of chick embryos at stages 13 to 15 or into the right hind limb buds of chick embryos at stages 18 to 20; the embryos were then allowed to develop for a total of 10, 15, or 18 days. Similar phenotypes were observed after infection at the different stages.

Infection with dnBMPR produced three major phenotypes: soft tissue syndactyly (webbing), transformation of scales to feathers, and truncation of the digits (Fig. 1). In essentially 100% of the infected limbs (n > 70), the interdigital tissue did not regress properly and thus the digits were joined by extensive webbing. Embryos examined as late as days 15 and 18 showed persistence of webbing (*20*). We never observed fusion of the digits or ectopic cartilage nodules in the infected foot plates. Extensive webbing was observed in limbs in which the digits were not truncated (Fig. 1, A and B) (*20*), thus indicating that the absence of cell death is not due to an inhibition of growth or cartilage differentiation (*21*). Control infections with RCAS encoding alkaline

Molecular Biology Program, Memorial Sloan-Kettering Cancer Center, 1275 York Avenue, New York, NY 10021, USA, and Graduate School of Medical Sciences, Cornell University, 445 East 69th Street, New York, NY 10021, USA.

*To whom correspondence should be addressed. E-mail: L-niswander@ski.mskcc.org